UC Berkeley
UC Berkeley Previously Published Works

Title

Next-Generation Cathode Materials for Non-aqueous Potassium-Ion Batteries

Permalink

https://escholarship.org/uc/item/1z44d7t4

Journal

Trends in Chemistry, 1(7)

ISSN

2589-7209

Authors

Kim, Haegyeom
Ji, Huiwen
Wang, Jingyang
et al.

Publication Date

2019-10-01

DOI

10.1016/j.trechm.2019.04.007

Peer reviewed

Next-generation cathode materials for non-aqueous potassium-ion batteries

Haegyeom Kim[a†], Huiwen Ji[b†], Jingyang Wang[b] and Gerbrand Ceder[a, b*]

a. Materials Science Division, Lawrence Berkeley National Laboratory, Berkeley, CA 94720, USA

b. Department of Materials Science and Engineering, University of California, Berkeley, CA 94720, USA

[†] These authors contributed equally to this work

[*] Email: gceder@berkeley.edu (G. Ceder)

Abstract

Potassium-ion batteries have recently attracted considerable attention as cost-effective alternatives to lithium-ion batteries for large-scale energy storage. However, a major obstacle to the practical application of this emerging technology is the lack of suitable cathode materials that are capable of delivering high gravimetric/volumetric energy, stable cycle life, and high rate capability. In this article, we review the recent progress in cathodes development for potassium-ion batteries. These materials are categorized into four types: layered oxides, Prussian blue analogues, poly-anion and organic compounds. Based on our critical review of the reported literature, we identify poly-anion compounds as a class of promising candidates among all types and provide suggestions for future optimization.

Keywords: Potassium; batteries; energy storage; cathodes; poly-anion; intercalation.

Potassium-ion batteries as next-generation energy-storage systems

Despite being the dominant energy storage solution for portable electronics, lithium-ion batteries (LIBs) face challenges in terms of cost for large-scale applications, including electric vehicles and stationary storage[1]. Currently, the cost of the active cathode and anode materials in LIBs can reach nearly 40% of the total cell cost [2]. In addition, the costs are subject to resource constraints resulting from the reliance on lithium and cobalt sources for the cathode materials [1]. Compared with Li, other alkali metals such as Na and K have the advantages of being significantly less expensive (Figure 1a) [3], and their storage can often be achieved with cathode materials that do not contain resource-constrained metals [4-11].

Both Na-ion batteries (NIBs) [12-15] and K-ion batteries (KIBs) [16-19] have been actively investigated as alternative energy-storage systems. In particular, KIBs are more attractive because: (1) graphite can be used as the anode for KIBs (unlike for NIBs) [20]; (2) KIB cathodes rely on almost completely different chemistries than Li-cathodes, which can lead to less expensive Co-free batteries, often based on transition metal(TM) elements such as Fe, Mn, and V (Figure 1b); (3) KIBs can potentially have higher voltages because the standard redox potential of K^+/K (–2.93 V *vs.* the

standard hydrogen electrode (SHE)) is comparable to that of Li^+/Li (–3.04 V *vs.* SHE) and lower than that of Na^+/Na (–2.71 V *vs.* SHE – in fact, the redox potential of K^+/K can be even lower than that of Li^+/Li [20]; (4) The K^+ mobility in electrolytes is higher than that of Li^+ or Na^+ [21]; and (5) finally, less expensive Al current collectors can be used for KIBs.

However, a major challenge for the practical realization of KIBs is the identification of a suitable cathode that reversibly intercalates K^+ ions with high capacity, suitable voltage, fast kinetics, and reliable cycle life. Because the ionic radius of K^+ is significantly larger than that of Li^+, K^+ ions often stabilize different structure types than Li^+. Consequently, the corresponding cathode materials and their working voltages are expected to be different from those for LIBs. The various material types that have been developed and evaluated as cathodes for non-aqueous KIBs since 2004 (Figure 1c) fall mainly into four categories: layered oxides, Prussian blue analogues (PBAs), poly-anion oxides, and organic compounds. Their capacity and voltage range are plotted in Figure 1d. Noticeably, the dominating cathode materials for LIBs are no longer the superior choice for KIBs. Instead, PBAs, which are poor-performing Li-ion cathodes, emerge as one of the major candidate material groups for KIBs when prioritized in terms of specific energy.

In this article, we review recent progress in the development of cathode materials for non-aqueous KIBs, with the aim of stimulating further research in this rapidly growing field. We first discuss the advantages and

disadvantages of each of the four cathode material types and provide perspectives and strategies for their future optimization.

Layered oxide compounds

Layered oxide compounds have been widely used as cathodes for LIBs and NIBs because of their high energy density achieved in these technologies. The layered oxides can be conveniently classified using an alpha-numeric expression developed by Delmas and colleagues [22]: with a letter describing the alkali site coordination (e.g., octahedral (O) or prismatic (P)) and a number referring to the oxygen stacking sequence. In a layered oxide crystal structure, the TM and alkali ions segregate into alternating slabs, forming a two-dimensional open framework for the fast migration of alkali ions, including the large K^+ ions, making them likely candidates for K storage compounds.

$K_{0.3}MnO_2$ was the first layered compound demonstrated as a suitable cathode for K storage [23]. It adopts a distorted P2-type structure with orthorhombic symmetry (space group: C*mcm*). When cycled between 1.5–4.0 V, the material delivers a reversible capacity of ~125 mAh g^{-1}. Since then, many more layered K-cathodes have emerged. For instance, Kim and colleagues developed a P3-type $K_{0.5}MnO_2$ cathode, which showed a reversible capacity of ~110 mAh g^{-1} between 1.5–3.9 V [5]. Significant capacity increase to ~140 mA h g^{-1} was observed when cycled to a higher upper cut-off voltage of 4.2 V, yet accompanied by fast capacity decay. The K_xCoO_2 reported by Kim and

4

colleagues [24] and Hironaka and colleagues [25] shows two structure types (*i.e.* P2 and P3) depending on the starting alkali content (x = ~0.4 and ~0.6, respectively). The P2-type K_xCoO_2 shows a stair-like charge/discharge profile, indicating the occurrence of multiple phase transitions upon K de/intercalation (Figure 2a), as confirmed by *in situ* X-ray diffraction (XRD) characterization. Hironaka and colleagues demonstrated that the voltage curves of K_xCoO_2 are not significantly affected by the oxygen stacking sequence (P2 *vs.* P3) of the as-synthesized pristine material [25]. Instead, both authors argue that the voltage profiles are dominated by K^+/vacancy ordering. Recently, a P2-type $K_2Ni_2TeO_6$ cathode was reported by Masese and colleagues [26]. This material has a high average discharge voltage of ~3.3 V but a low reversible capacity of ~65 mAh g^{-1}. The authors attributed the high working voltage to the electro-negative TeO_6^{6-} moieties. The effect of mixed TMs on cathode performance has also been investigated. These mixed-TM oxides (*i.e.* $K_xFe_{0.5}Mn_{0.5}O_2$) [4] deliver higher specific capacity than single-TM oxides (e.g., K_xMnO_2 and K_xCoO_2). Nevertheless, no significant improvement in the energy density was observed because of the decrease in the operating voltage.

One of the major issues with layered oxides is that almost all of them are K-deficient, limiting the amount of K that they can bring in a K cell. In this context, the stoichiometric O3-type $KCrO_2$ developed by Kim and colleagues is remarkable as it is the only layered oxide material that can be synthesized without K deficiency [27]. A stoichiometric O3-type $KCrO_2$ shows a reversible

capacity of ~93 mAh g^{-1} with an average voltage of ~2.73 V (Figure 2b) [27]. The unique stability of $KCrO_2$ in the layered structure (Figure 2c) was explained using *ab-initio* calculations. By evaluating the thermodynamic stability of various stoichiometric KMO_2 compounds (Figure 2c), Kim and colleagues [27] found that the strong unscreened K^+–K^+ interactions destabilize the layered structure for most stoichiometric KMO_2 compounds and instead favor other three-dimensional structures. However, the strong octahedral site preference of Cr^{3+} can overcome the penalty of the K^+–K^+ interactions, thereby uniquely stabilizing $KCrO_2$ in the layered structure.

Another major drawback of layered K-compounds is their much steeper voltage curves with many more voltage steps compared to those of corresponding Li and Na systems (Figure 2d) [25]. For example, while O2-$LiCoO_2$ exhibits a flat voltage profile [25, 28], a steeper voltage profile with multiple steps is observed for P2-$Na_{2/3}CoO_2$. These slope features become even more apparent in P2-$K_{0.41}CoO_2$. P2-Na_xCoO_2 exhibits 8 voltage steps between $Na_{0.1}CoO_2$ and $Na_{0.65}CoO_2$, which on average equals one voltage step for every 0.069 Na ion intercalated; whereas P2-K_xCoO_2 has 7 voltage steps between $K_{0.2}CoO_2$ and $K_{0.5}CoO_2$, which equals one voltage step for every 0.043 K ion intercalated. The underlying mechanism is that as the alkali ions become larger, the increasing inter-slab distance prevents the oxygen anions from effectively screening the alkali–alkali repulsion, leading to a stronger interaction between them. Such strong and long-ranged repulsive interactions cause a remarkable number of phase transitions between

6

various ordered K^+-vacancy configurations, as well as large voltage slope. The relation between voltage slope and interaction can be seen by taking the derivative of $V(x) = -\mu_K(x) \approx \frac{\delta E}{\delta x}$, where x is the amount of K.[29] In a mean field or regular solution approach, $\Delta E_{mix} = \omega x(1-x)$ and hence $\frac{\delta V(x)}{\delta x} \approx -2\omega$, , where ω is proportional to the effective K-K interaction.[30] Even in systems where the intercalating ions are not randomly distributed, the overall slope remains proportional to the interaction. The large voltage slope limits the usable capacity within a given voltage window.

In addition, the upper cutoff voltage allowed for most K-layered oxides is limited due to the structural instability and the concomitant capacity loss at deep charge [5, 23-25, 27]. For example, when depotassiating K_xMnO_2 and K_yCrO_2 to x < 0.2 and y < 0.4, respectively, the crystallinity of electrodes is significantly reduced [5, 27] as confirmed by *ex situ* XRD. The origin of this irreversible structural change at low K contents is currently unclear and should be further investigated to enable the use of a wider K de/intercalation range.

Prussian blue analogues

Prussian blue analogues (PBAs) have received considerable attention as K-cathode materials because of their long cycle life, inexpensive TM components, and potentially scalable synthesis. Their three-dimensional (3D)

open frameworks (Figure 3a) host reversible redox reactions by allowing the insertion/extraction of alkali ions. The composition of a PBA can be expressed as $K_xM_A[M_B(CN)_6]_{1-\delta} \cdot nH_2O$, where M_A and M_B denote the N-coordinated and C-coordinated TM ions, respectively, and δ and n denote the contents of $[M_B(CN)_6]$ vacancies and residual water, respectively. Initially, PBAs were used as both anode and cathode in aqueous electrolytes [31]; however, the limited variation of redox potential that can be realized in PBAs leads to a limited battery voltage. In 2004, Eftekhari first demonstrated the use of electrochemically deposited $KFe[Fe(CN)_6]$ as a K-cathode in a nonaqueous electrolyte, achieving a high voltage of ~3.7 V (*vs.* K^+/K) and a reasonable capacity of ~0.9 K/f.u. (formula unit) [32]

The specific capacity of K-PBAs is slightly lower than that of Na-PBAs because of the heavier K^+ ions; nevertheless, their higher voltages result in competitive specific energies (Figure 3b) [8-10, 33-39]. There are two known factors that contribute to the voltage difference: (1) the lower anode potential for K^+/K than for Na^+/Na, and (2) according to density functional theory [40], the interaction between alkali ions and the metal–organic framework strengthens with alkali size, which stabilizes the discharged products and results in an increasing intercalation potential from Li^+ to Na^+ to K^+. The voltages of Li-PBAs are comparable to those of Na-PBAs most likely because of the cancellation of these two effects. The increased voltage with increasing ionic radius of intercalating species may also explain why $Co^{2+/3+}$ is redox-active for Na-PBAs but has a redox potential above the upper

stability window of non-aqueous electrolytes for K-PBAs [33]. Thus, the only K-PBAs capable of delivering a capacity larger than 1 K/f.u. at reasonably high voltage are either Fe- or Mn-based [11, 34].

The electrochemical performance of PBAs is highly sensitive to lattice defects. A PBA can theoretically insert/extract 2 K/f.u., corresponding to a theoretical capacity of ~156 mAh g^{-1}. However, the [Fe(CN)$_6$] vacancies and residual water negatively affect the electrochemical performance. The former reduces the available electron reservoir, and the latter leads to side reactions and low coulombic efficiency. For example, K$_{0.220}$Fe[Fe(CN)$_6$]$_{0.805}$·4.01H$_2$O which has a high vacancy and water content as a result of its rapid precipitation synthesis delivers a capacity of ~0.84 K/f.u. with low initial coulombic efficiency of 44% [41]. Slow crystallite nucleation and post-synthesis drying seem critical for better performance [42]. A similar study comparing the effect of crystallinity on performance in Na-PBAs concluded that defects lead to slow kinetics and poor cycle life [43].

Such sensitivity to defects leads to significant inconsistencies across the literature. A wide spectrum of synthesis methods and conditions have been reported, yielding varied electrochemical results even for the same PBA system. Chong and colleagues reported moderate rate performance for nanosized KFe[Fe(CN)$_6$]$_{0.82}$·2.87H$_2$O prepared using hydrothermal synthesis [9]. In contrast, Shadike and colleagues reported superior rate capability for a K-deficient phase FeFe(CN)$_6$ (the actual composition was not reported) synthesized using a simple precipitation method [10]. This high rate

capability was tentatively attributed to the minimal structural deformation during cycling. The voltage profiles also vary. $K_{0.61}Fe[Fe(CN)_6]_{0.91}\cdot0.32H_2O$ reported by Zhu and colleagues has a significantly longer discharge plateau at 3.28 V than at 3.95 V (Figure 3c) [44]; in contrast, $K_{1.64}Fe[Fe(CN)_6]_{0.89}\cdot0.15H_2O$ reported by Bie and colleagues shows two equally long discharge plateaus at 3.8 and 3.15 V (Figure 3d) [34]; and the K-deficient $FeFe(CN)_6$ phase reported by Shadike and colleagues has two almost overlapping plateaus at 3.3 and 3.2 V (Figure 3e) [10]. No real satisfactory explanations for these variations have been provided so far.

Such confusion is in fact not uncommon in the field of metal–organic frameworks (MOFs), where routine measurements such as powder XRD provide limited structural information to explain the observed variation in properties [45]. In-depth characterization of the nature of the defects using theory and experiments and their correlation with electrochemical performance is urgently needed. This understanding needs to be paired with study of how synthetic conditions influence composition and defects to increase reproducibility and future optimization/commercialization of this class of materials.

Polyanionic compounds

Polyanionic compounds have also been investigated as high-voltage cathodes for KIBs. Recham and colleagues demonstrated reversible K de/intercalation in polyanion compounds [46]. They first extracted ~0.9 K^+/f.u. from a $KFeSO_4F$ electrode using $Li/KFeSO_4F$ cells. The depotassiated

material was subsequently evaluated in K/FeSO$_4$F cells and ~0.8 K$^+$/f.u. could be reintercalated at an average voltage of ~3.6 V. Later, an extensive screening of known K-containing compounds in the K-M-O and K-M-P-O space was conducted by Park and colleagues based on several criteria, including [47]: the material contains oxidizable TM species (e.g., Ti, V, Cr, Mn, Fe, Co, Ni, and Mo) in octahedral sites; the material has one-dimensional K$^+$ transport channels with large void space (> 1.8 Å); and the theoretical capacity is larger than 80 mAh g^{-1}. The screening identified 10 candidates, including KMP$_2$O$_7$ (M = Ti, V, Cr, Fe, Mo), KM(PO$_3$)$_3$ (M = Ni, Co), K$_2$(VO$_3$)(P$_2$O$_7$)$_2$, K$_2$MnP$_2$O$_7$, and KMnVO$_4$. Among them, only KMP$_2$O$_7$ (M = Ti, V, and Mo) shows reversible capacity during galvanostatic cycling: KTiP$_2$O$_7$ and KMoP$_2$O$_7$ have limited capacities (~20 mAh g^{-1}) and low average voltages (< 3.0 V) even at 50 °C, while KVP$_2$O$_7$ exhibits reasonable electrochemical performance, delivering ~55 mAh g^{-1} at ~4.2 V (Figure 4a) [47]. The structural evolution of KVP$_2$O$_7$ during cycling detected using *in situ* and *ex situ* XRD suggested a reversible two-phase reaction between the monoclinic KVP$_2$O$_7$ and the triclinic K$_{0.4}$VP$_2$O$_7$. Recently, two new high-voltage cathodes, KVPO$_4$F and KVOPO$_4$, were investigated by Chihara and colleagues [48], which achieved capacities of ~92 and 84 mAh g^{-1} with average voltages of ~4.13 and ~4.0 V, respectively. The average voltage and capacity of KVPO$_4$F were further improved by Kim and colleagues to ~4.33 V and ~105 mAh g^{-1}, respectively, through the synthesis of a highly stoichiometric compound (Figure 4b) [49]. Their structure analysis using XRD, X-ray absorption

spectroscopy, and nuclear magnetic resonance spectroscopy showed that oxygen substitution on F sites in $KVPO_4F$ induces anion-disordering, thus reducing the working voltage and specific capacity. Their findings suggest that the material prepared by Chihara and colleagues [48] was likely an oxygen-substituted $KVPO_{4+x}F_{1-x}$ compound, which explains the origin of its lower voltage and capacity than a stoichiometric $KVPO_4F$. Kim and colleagues thus proposed that the synthesis of stoichiometric $KVPO_4F$ is crucial to achieving high voltage and capacity.

Metastable K-containing polyanionic compounds have also been obtained and evaluated. A $K_3V_2(PO_4)_2F_3$ cathode was prepared *via* electrochemical Na^+/K^+ exchange from a NASICON-type $Na_3V_2(PO_4)_2F_3$ by Lin and colleagues [50]. *In situ* XRD and *ex situ* energy-dispersive X-ray spectroscopy (EDX) analysis revealed the complete replacement of Na^+ ions with K^+ ions after 5 cycles. The *in situ* formed $K_3V_2(PO_4)_2F_3$ cathode provides a reversible capacity of ~103 mAh g^{-1}, corresponding to ~1.8 K^+/f.u., with an average voltage of ~3.75 V (Figure 4c). The performance is similar to that of $Na_3V_2(PO_4)_2F_3$, which de/intercalates 2 Na^+/f.u. at an average voltage of 3.8 V [51]. An attempt to directly synthesize $K_3V_2(PO_4)_2F_3$ using a conventional solid-state method was not successful [50].

In general, most polyanionic compounds provide higher voltages (>3.5 V *vs.* K/K^+) than Na-analogues and are even comparable to some Li-analogues [46-60], with some materials cycling at over 4.0 V *vs.* K/K^+ (*i.e.,* KVP_2O_7, $KVPO_4F$, and $KVOPO_4$) as shown in Figure 4d [47-49]. The high voltage of polyanionic

compounds can be attributed to three factors: (1) the inductive effect of the electro-negative polyanion moieties, (2) a 3D K arrangements with larger K^+-K^+ distances than in layered oxides which reduces the effective K^+-K^+ interaction, and (3) a 3D framework in which the volume change associated with K-insertion is spread out between all three dimensions, unlike in layered materials where it is largely accommodated by slab-space expansion which compromises the screening of K^+-K^+ interaction. It is worth noting that the 3rd factor may not be present when the polyanion compound has a layered structure that can easily relax perpendicular to the layer. However, the specific capacity of many K-polyanionic compounds is still far below Li- and Na-counterparts. We propose that new polyanionic K-cathodes that enable double redox reactions (e.g., $Mn^{2+/4+}$, $V^{3+/5+}$, and $Ni^{2+/4+}$) should be developed to increase the theoretical electron reservoir.

Organic compounds

Organic compounds are considered attractive candidates for KIBs by some because of their low cost and flexible structures. The argument made is that weak intermolecular interaction more easily accommodates deformations upon inserting large K^+ ions. PTCDA (3,4,9,10-perylene-tetracarboxylic acid-dianhydride) was first demonstrated by Chen and colleagues as a cathode material and exhibits a capacity of 131 mAh g^{-1} in the voltage range of 1.5–3.5 V, corresponding to the insertion of 2 K^+/f.u. [61]. Xing and colleagues evaluated the structural evolution of PTCDA using *ex situ* XRD [62] and

showed that the material undergoes a high degree of amorphization upon potassiation with its crystallinity only partially restored when re-charged. We suspect that this loss of long-range order is responsible for the poor cycling stability, though it is not exactly clear why amorphization would reduce capacity. In addition, *ex situ* infrared spectra reveals electron injection into C=O bonds and the formation of potassium enolate groups during the potassiation process. However, the authors suggested that the redox process is better described by a molecular orbital or doping analogy because of the delocalized nature of the injected electrons. Jian and colleagues studied PAQS (poly(anthraquinonyl sulfide)) as another cathode material for KIBs [63]. This compound shows a high reversible capacity of 200 mAh g^{-1} and good cycling performance with 75% of the initial capacity retained after 50 cycles at a rate of C/10. A series of oxocarbon salts with the formula $K_2(CO)_n$ (n = 4, 5, 6), were investigated by Zhao and colleagues as KIB cathodes [64]. These materials deliver a capacity of 212 mAh g^{-1} at 0.2C and 164 mAh g^{-1} at 10C, and the two-electron reaction mechanism of the carbonyl group was confirmed by *in situ* Raman measurements. Very recently, CuTCNQ (copper-tetracyanoquinodimethane) was proposed as a cathode material for KIBs with a discharge capacity of 244 mAh g^{-1} at an average discharge potential of 2.7 V, utilizing both redox-active $Cu^{+/2+}$ and $TCNQ^{2-/0}$ [65]. However, it should be noted that, in this work, the $TCNQ^{2-/0}$ redox process is accompanied by anion insertion from electrolytes, rendering the material unsuitable for realizing practical rocking-chair-type KIBs because the anions

in the electrolytes are cycled during battery operation. In summary, the rich and versatile chemistry of organic compounds can potentially offer a cost-efficient solution for KIBs; however, several issues must be properly addressed: the low volumetric energy density and low operating voltage of most organic systems will have to be compensated by other benefits achieved when using organic cathodes. Dissolution of organic species from the cathode in conventional organic electrolytes result in poor capacity retention. In addition, organic cathodes themselves usually do not contain K^+ ions; therefore, the need for a pre-potassiation process or the use of a K metal anode are additional drawbacks for their practical application.

Concluding Remarks and Future Perspectives

In Figure 5, the gravimetric energy is plotted versus the volumetric energy of various K-cathode compounds, including layered compounds, Prussian analogues, polyanionic compounds, and organic compounds with comparison to Li- and Na-cathode materials [11, 24, 26, 27, 35, 39, 46, 49, 57, 60, 61, 63, 66-71]. A few K-cathode materials (e.g., $KVPO_4F$) [49] exhibit comparable gravimetric and volumetric energies to Na cathode materials. However, most of the K cathodes still have lower energy content, especially volumetrically, than Li or Na cathode materials.

The large ionic radius of K^+ leads to very different structural requirements for cathode materials than for Li^+. Layered oxide compounds, which have a two-dimensional arrangement of K^+ ions, poorly screen the strong K^+–K^+

interactions, resulting in a significantly more sloped voltage profile and low specific energy (<300 Wh kg^{-1}) than Li- or Na-based layered oxides. In contrast, PBAs and polyanionic compounds have three-dimensional K arrangements, which can effectively reduce K$^+$–K$^+$ interactions. Therefore, PBAs and polyanionic compounds have flatter voltage profiles and higher average working voltage and thus deliver higher gravimetric energy. For example, KVPO$_4$F provides ~450 Wh kg^{-1} and K$_2$MnFe(CN)$_6$ delivers ~510 Wh kg^{-1}[11, 49]. These examples indicate that PBAs and polyanionic compounds are promising material classes in which to find better cathodes with high specific energy. Likewise, any search for new materials should focus on three-dimensional structures. Some important challenges are listed in the Outstanding Questions section.

Future endeavors in optimizing PBA and polyanionic structures should focus on addressing their specific limitations. Despite the high gravimetric energy (> 450 Wh kg^{-1}) of PBAs, they exhibit low energy density (< 1200 Wh L^{-1}). Some investigation in the role of the interstitial water molecules in PBAs is needed as its content is difficult to precisely control and it remains unclear how the interstitial water molecules in PBAs lead to deterioration of their capacity with cycling. We expect that polyanionic compounds are better options for KIB cathodes. They have higher volumetric energy density and less complex structures and fewer defects (i.e., interstitial water and TM vacancy in the structure) than PBAs. Though several K-polyanionic compounds with high working voltage (>3.5 V) have been developed, their

16

energy density is not yet sufficient to compete with most Li and Na cathodes. To increase the energy density of KIBs, K polyanionic cathodes that can enable double redox reactions (i.e., $Mn^{2+/4+}$, $V^{3+/5+}$, and $Ni^{2+/4+}$) should be developed to increase the achievable specific capacity. Given that polyanionic compounds are generally high in voltage, strategies to optimize the working potential in order to fully utilize double redox in a practical voltage window are needed, e.g. tuning the inductive effect by tailoring the polyanionic groups, or by tailoring the site energy.

Conflict of interest statement

The authors declare that there is no conflict of interest.

Acknowledgments

References

1.   Olivetti, E.A., Ceder, G., Gaustad, G.G., and Fu, X. (2017). Lithium-Ion Battery Supply Chain Considerations: Analysis of Potential Bottlenecks in Critical Metals. Joule *1*, 229-243.
2.   Chung, D., Elgqvist, E., and Santhanagopalan, S. (2015). Automotive Lithium-ion Battery Supply Chain and US Competitiveness Considerations (Clean Energy Manufacturing Analysis Center (CEMAC)).

3.   USGS Minerals Information: Commodity Statistics and Information (https://minerals.usgs.gov/minerals/pubs/commodity/) Accessed October 2018.

4.   Wang, X., Xu, X., Niu, C., Meng, J., Huang, M., Liu, X., Liu, Z., and Mai, L. (2017). Earth Abundant Fe/Mn-Based Layered Oxide Interconnected Nanowires for Advanced K-Ion Full Batteries. Nano Lett *17*, 544-550.

5.   Kim, H., Seo, D.-H., Kim, J.C., Bo, S.-H., Liu, L., Shi, T., and Ceder, G. (2017). Investigation of Potassium Storage in Layered P3-Type K0.5MnO2 Cathode. Adv Mater *29*, 1702480.

6.   Deng, T., Fan, X., Chen, J., Chen, L., Luo, C., Zhou, X., Yang, J., Zheng, S., and Wang, C. (2018). Layered P2-Type K0.65Fe0.5Mn0.5O2 Microspheres as Superior Cathode for High-Energy Potassium-Ion Batteries. Adv Funct Mater *28*, 1800219.

7.   Zhao, S., Yan, K., Munroe, P., Sun, B., and Wang, G. (2019). Construction of Hierarchical K1.39Mn3O6 Spheres via AlF3 Coating for High-Performance Potassium-Ion Batteries. Adv Energy Mater *9*, 1803757.

8.   Pei, Y., Mu, C., Li, H., Li, F., and Chen, J. (2018). Low-Cost K4Fe(CN)6 as a High-Voltage Cathode for Potassium-Ion Batteries. ChemSusChem *11*, 1285-1289.

9.   Chong, S., Chen, Y., Zheng, Y., Tan, Q., Shu, C., Liu, Y., and Guo, Z. (2017). Potassium ferrous ferricyanide nanoparticles as a high capacity and ultralong life cathode material for nonaqueous potassium-ion batteries. J Mater Chem A *5*, 22465-22471.

10.   Shadike, Z., Shi, D.-R., Tian, W., Cao, M.-H., Yang, S.-F., Chen, J., and Fu, Z.-W. (2017). Long life and high-rate Berlin green FeFe(CN)6 cathode material for a non-aqueous potassium-ion battery. J Mater Chem A *5*, 6393-6398.

11.   Xue, L., Li, Y., Gao, H., Zhou, W., Lü, X., Kaveevivitchai, W., Manthiram, A., and Goodenough, J.B. (2017). Low-Cost High-Energy Potassium Cathode. J Am Chem Soc *139*, 2164-2167.

12.   Kim, H., Kim, H., Ding, Z., Lee, M.H., Lim, K., Yoon, G., and Kang, K. (2016). Recent Progress in Electrode Materials for Sodium-Ion Batteries. Adv Energy Mater *6*, 1600943.

13.   Kim, S.-W., Seo, D.-H., Ma, X., Ceder, G., and Kang, K. (2012). Electrode Materials for Rechargeable Sodium-Ion Batteries: Potential Alternatives to Current Lithium-Ion Batteries. Adv Energy Mater *2*, 710-721.

14.   Chevrier, V.L., and Ceder, G. (2011). Challenges for Na-ion Negative Electrodes. J Electrochem Soc *158*, A1011-A1014.

15.   Palomares, V., Serras, P., Villaluenga, I., Hueso, K.B., Carretero-González, J., and Rojo, T. (2012). Na-ion batteries, recent advances and present challenges to become low cost energy storage systems. Energy Environ Sci *5*, 5884-5901.

16.   Kim, H., Kim, J.C., Bianchini, M., Seo, D.-H., Rodriguez-Garcia, J., and Ceder, G. (2018). Recent Progress and Perspective in Electrode Materials for K-Ion Batteries. Adv Energy Mater *8*, 1702384.

17.	Wu, X., Leonard, D.P., and Ji, X. (2017). Emerging Non-Aqueous Potassium-Ion Batteries: Challenges and Opportunities. Chem Mater *29*, 5031-5042.

18.	Pramudita, J.C., Sehrawat, D., Goonetilleke, D., and Sharma, N. (2017). An Initial Review of the Status of Electrode Materials for Potassium-Ion Batteries. Adv Energy Mater *7*, 1602911.

19.	Eftekhari, A., Jian, Z., and Ji, X. (2017). Potassium Secondary Batteries. ACS Appl Mater Intf *9*, 4404-4419.

20.	Komaba, S., Hasegawa, T., Dahbi, M., and Kubota, K. (2015). Potassium intercalation into graphite to realize high-voltage/high-power potassium-ion batteries and potassium-ion capacitors. Electrochem Commun *60*, 172-175.

21.	Okoshi, M., Yamada, Y., Komaba, S., Yamada, A., and Nakai, H. (2017). Theoretical Analysis of Interactions between Potassium Ions and Organic Electrolyte Solvents: A Comparison with Lithium, Sodium, and Magnesium Ions. J Electrochem Soc *164*, A54-A60.

22.	Delmas, C., Fouassier, C., and Hagenmuller, P. (1980). Structural classification and properties of the layered oxides. Physica B+C *99*, 81-85.

23.	Vaalma, C., Giffin, G.A., Buchholz, D., and Passerini, S. (2016). Non-Aqueous K-Ion Battery Based on Layered K0.3MnO2 and Hard Carbon/Carbon Black. J Electrochem Soc *163*, A1295-A1299.

24.	Kim, H., Kim, J.C., Bo, S.-H., Shi, T., Kwon, D.-H., and Ceder, G. (2017). K-Ion Batteries Based on a P2-Type K0.6CoO2 Cathode. Adv Energy Mater *7*, 1700098.

25.	Hironaka, Y., Kubota, K., and Komaba, S. (2017). P2- and P3-KxCoO2 as an electrochemical potassium intercalation host. Chem Commun *53*, 3693-3696.

26.	Masese, T., Yoshii, K., Yamaguchi, Y., Okumura, T., Huang, Z.-D., Kato, M., Kubota, K., Furutani, J., Orikasa, Y., Senoh, H.*, et al.* (2018). Rechargeable potassium-ion batteries with honeycomb-layered tellurates as high voltage cathodes and fast potassium-ion conductors. Nat Commun *9*, 3823.

27.	Kim, H., Seo, D.-H., Urban, A., Lee, J., Kwon, D.-H., Bo, S.-H., Shi, T., Papp, J.K., McCloskey, B.D., and Ceder, G. (2018). Stoichiometric Layered Potassium Transition Metal Oxide for Rechargeable Potassium Batteries. Chem Mater *30*, 6532-6539.

28.	Yabuuchi, N., Kawamoto, Y., Hara, R., Ishigaki, T., Hoshikawa, A., Yonemura, M., Kamiyama, T., and Komaba, S. (2013). A Comparative Study of LiCoO2 Polymorphs: Structural and Electrochemical Characterization of O2-, O3-, and O4-type Phases. Inorg Chem *52*, 9131-9142.

29.	Aydinol, M.K., and Ceder, G. (1997). First-Principles Prediction of Insertion Potentials in Li-Mn Oxides for Secondary Li Batteries. J Electrochem Soc *144*, 3832-3835.

30.	Bevan Ott, J., and Boerio-Goates, J. (2000). Preface to the Two-Volume Series: Chemical Thermodynamics: Principles and Applications and Chemical Thermodynamics: Advanced Applications. In Chemical Thermodynamics: Principles and Applications, J.B. Ott, and J. Boerio-Goates, eds. (London: Academic Press), pp. xv-xix.

31. Jayalakshmi, M., and Scholz, F. (2000). Charge–discharge characteristics of a solid-state Prussian blue secondary cell. J Power Sources *87*, 212-217.

32. Eftekhari, A. (2004). Potassium secondary cell based on Prussian blue cathode. J Power Sources *126*, 221-228.

33. Wu, X., Jian, Z., Li, Z., and Ji, X. (2017). Prussian white analogues as promising cathode for non-aqueous potassium-ion batteries. Electrochem Commun *77*, 54-57.

34. Bie, X., Kubota, K., Hosaka, T., Chihara, K., and Komaba, S. (2017). A novel K-ion battery: hexacyanoferrate(ii)/graphite cell. J Mater Chem A *5*, 4325-4330.

35. Song, J., Wang, L., Lu, Y., Liu, J., Guo, B., Xiao, P., Lee, J.-J., Yang, X.-Q., Henkelman, G., and Goodenough, J.B. (2015). Removal of Interstitial H2O in Hexacyanometallates for a Superior Cathode of a Sodium-Ion Battery. J Am Chem Soc *137*, 2658-2664.

36. Wang, B., Han, Y., Wang, X., Bahlawane, N., Pan, H., Yan, M., and Jiang, Y. (2018). Prussian Blue Analogs for Rechargeable Batteries. iScience *3*, 110-133.

37. Wang, L., Song, J., Qiao, R., Wray, L.A., Hossain, M.A., Chuang, Y.-D., Yang, W., Lu, Y., Evans, D., Lee, J.-J., *et al.* (2015). Rhombohedral Prussian White as Cathode for Rechargeable Sodium-Ion Batteries. J Am Chem Soc *137*, 2548-2554.

38. Mizuno, Y., Okubo, M., Kagesawa, K., Asakura, D., Kudo, T., Zhou, H., Oh-ishi, K., Okazawa, A., and Kojima, N. (2012). Precise Electrochemical Control of Ferromagnetism in a Cyanide-Bridged Bimetallic Coordination Polymer. Inorg Chem *51*, 10311-10316.

39. Okubo, M., Asakura, D., Mizuno, Y., Kim, J.D., Mizokawa, T., Kudo, T., and Honma, I. (2010). Switching Redox-Active Sites by Valence Tautomerism in Prussian Blue Analogues AxMny[Fe(CN)6]·nH2O (A: K, Rb): Robust Frameworks for Reversible Li Storage. J Phys Chem Lett *1*, 2063-2071.

40. Ling, C., Chen, J., and Mizuno, F. (2013). First-Principles Study of Alkali and Alkaline Earth Ion Intercalation in Iron Hexacyanoferrate: The Important Role of Ionic Radius. J Phys Chem C *117*, 21158-21165.

41. Zhang, C., Xu, Y., Zhou, M., Liang, L., Dong, H., Wu, M., Yang, Y., and Lei, Y. (2017). Potassium Prussian Blue Nanoparticles: A Low-Cost Cathode Material for Potassium-Ion Batteries. Adv Funct Mater *27*, 1604307.

42. He, G., and Nazar, L.F. (2017). Crystallite Size Control of Prussian White Analogues for Nonaqueous Potassium-Ion Batteries. ACS Energy Lett *2*, 1122-1127.

43. You, Y., Wu, X.-L., Yin, Y.-X., and Guo, Y.-G. (2014). High-quality Prussian blue crystals as superior cathode materials for room-temperature sodium-ion batteries. Energy Environ Sci *7*, 1643-1647.

44. Zhu, Y.-H., Yang, X., Bao, D., Bie, X.-F., Sun, T., Wang, S., Jiang, Y.-S., Zhang, X.-B., Yan, J.-M., and Jiang, Q. (2018). High-Energy-Density Flexible Potassium-Ion Battery Based on Patterned Electrodes. Joule *2*, 736-746.

45. Hafizovic, J., Bjørgen, M., Olsbye, U., Dietzel, P.D.C., Bordiga, S., Prestipino, C., Lamberti, C., and Lillerud, K.P. (2007). The Inconsistency in Adsorption Properties and Powder XRD Data of MOF-5 Is Rationalized by Framework Interpenetration and the Presence of Organic and Inorganic Species in the Nanocavities. J Am Chem Soc *129*, 3612-3620.

46. Recham, N., Rousse, G., Sougrati, M.T., Chotard, J.-N., Frayret, C., Mariyappan, S., Melot, B.C., Jumas, J.-C., and Tarascon, J.-M. (2012). Preparation and Characterization of a Stable FeSO4F-Based Framework for Alkali Ion Insertion Electrodes. Chem Mater *24*, 4363-4370.

47. Park, W.B., Han, S.C., Park, C., Hong, S.U., Han, U., Singh, S.P., Jung, Y.H., Ahn, D., Sohn, K.-S., and Pyo, M. (2018). KVP2O7 as a Robust High-Energy Cathode for Potassium-Ion Batteries: Pinpointed by a Full Screening of the Inorganic Registry under Specific Search Conditions. Adv Energy Mater *8*, 1703099.

48. Chihara, K., Katogi, A., Kubota, K., and Komaba, S. (2017). KVPO4F and KVOPO4 toward 4 volt-class potassium-ion batteries. Chem Commun *53*, 5208-5211.

49. Kim, H., Seo, D.-H., Bianchini, M., Clément, R.J., Kim, H., Kim, J.C., Tian, Y., Shi, T., Yoon, W.-S., and Ceder, G. (2018). A New Strategy for High-Voltage Cathodes for K-Ion Batteries: Stoichiometric KVPO4F. Adv Energy Mater *8*, 1801591.

50. Lin, X., Huang, J., Tan, H., Huang, J., and Zhang, B. (2019). K3V2(PO4)2F3 as a robust cathode for potassium-ion batteries. Energy Storage Mater *16*, 97-101.

51. Zhu, C., Wu, C., Chen, C.-C., Kopold, P., van Aken, P.A., Maier, J., and Yu, Y. (2017). A High Power–High Energy Na3V2(PO4)2F3 Sodium Cathode: Investigation of Transport Parameters, Rational Design and Realization. Chem Mater *29*, 5207-5215.

52. Liao, J., Hu, Q., Mu, J., He, X., Wang, S., and Chen, C. (2019). A vanadium-based metal–organic phosphate framework material K2[(VO)2(HPO4)2(C2O4)] as a cathode for potassium-ion batteries. Chem Commun *55*, 659-662.

53. Han, J., Li, G.-N., Liu, F., Wang, M., Zhang, Y., Hu, L., Dai, C., and Xu, M. (2017). Investigation of K3V2(PO4)3/C nanocomposites as high-potential cathode materials for potassium-ion batteries. Chem Commun *53*, 1805-1808.

54. Jian, Z., Han, W., Lu, X., Yang, H., Hu, Y.-S., Zhou, J., Zhou, Z., Li, J., Chen, W., Chen, D., *et al.* (2013). Superior Electrochemical Performance and Storage Mechanism of Na3V2(PO4)3 Cathode for Room-Temperature Sodium-Ion Batteries. Adv Energy Mater *3*, 156-160.

55. Jin, T., Liu, Y., Li, Y., Cao, K., Wang, X., and Jiao, L. (2017). Electrospun NaVPO4F/C Nanofibers as Self-Standing Cathode Material for Ultralong Cycle Life Na-Ion Batteries. Adv Energy Mater *7*, 1700087.

56. Barpanda, P., Oyama, G., Nishimura, S.-i., Chung, S.-C., and Yamada, A. (2014). A 3.8-V earth-abundant sodium battery electrode. Nat Commun *5*, 4358.

57.   Kang, B., and Ceder, G. (2009). Battery materials for ultrafast charging and discharging. Nature *458*, 190.

58.   Zheng, J.-c., Zhang, B., and Yang, Z.-h. (2012). Novel synthesis of LiVPO4F cathode material by chemical lithiation and postannealing. J Power Sources *202*, 380-383.

59.   Huang, H., Yin, S.-C., Kerr, T., Taylor, N., and Nazar, L.F. (2002). Nanostructured Composites: A High Capacity, Fast Rate Li3V2(PO4)3/Carbon Cathode for Rechargeable Lithium Batteries. Adv Mater *14*, 1525-1528.

60.   Ati, M., Melot, B.C., Chotard, J.N., Rousse, G., Reynaud, M., and Tarascon, J.M. (2011). Synthesis and electrochemical properties of pure LiFeSO4F in the triplite structure. Electrochem Commun *13*, 1280-1283.

61.   Chen, Y., Luo, W., Carter, M., Zhou, L., Dai, J., Fu, K., Lacey, S., Li, T., Wan, J., Han, X., *et al.* (2015). Organic electrode for non-aqueous potassium-ion batteries. Nano Energy *18*, 205-211.

62.   Xing, Z., Jian, Z., Luo, W., Qi, Y., Bommier, C., Chong, E.S., Li, Z., Hu, L., and Ji, X. (2016). A perylene anhydride crystal as a reversible electrode for K-ion batteries. Energy Storage Mater *2*, 63-68.

63.   Jian, Z., Liang, Y., Rodríguez-Pérez, I.A., Yao, Y., and Ji, X. (2016). Poly(anthraquinonyl sulfide) cathode for potassium-ion batteries. Electrochem Commun *71*, 5-8.

64.   Zhao, Q., Wang, J., Lu, Y., Li, Y., Liang, G., and Chen, J. (2016). Oxocarbon Salts for Fast Rechargeable Batteries. Angew Chem, Int Ed *55*, 12528-12532.

65.   Ma, J., Zhou, E., Fan, C., Wu, B., Li, C., Lu, Z.-H., and Li, J. (2018). Endowing CuTCNQ with a new role: a high-capacity cathode for K-ion batteries. Chem Commun *54*, 5578-5581.

66.   Berthelot, R., Carlier, D., and Delmas, C. (2010). Electrochemical investigation of the P2–NaxCoO2 phase diagram. Nat Mater *10*, 74.

67.   Yabuuchi, N., Kajiyama, M., Iwatate, J., Nishikawa, H., Hitomi, S., Okuyama, R., Usui, R., Yamada, Y., and Komaba, S. (2012). P2-type Nax[Fe1/2Mn1/2]O2 made from earth-abundant elements for rechargeable Na batteries. Nat Mater *11*, 512.

68.   Jian, Z., Zhao, L., Pan, H., Hu, Y.-S., Li, H., Chen, W., and Chen, L. (2012). Carbon coated Na3V2(PO4)3 as novel electrode material for sodium ion batteries. Electrochem Commun *14*, 86-89.

69.   Barker, J., Gover, R.K.B., Burns, P., Bryan, A., Saidi, M.Y., and Swoyer, J.L. (2005). Structural and electrochemical properties of lithium vanadium fluorophosphate, LiVPO4F. J Power Sources *146*, 516-520.

70.   Bianchini, M., Fauth, F., Brisset, N., Weill, F., Suard, E., Masquelier, C., and Croguennec, L. (2015). Comprehensive Investigation of the Na3V2(PO4)2F3–NaV2(PO4)2F3 System by Operando High Resolution Synchrotron X-ray Diffraction. Chem Mater *27*, 3009-3020.

71.   Ohzuku, T., and Ueda, A. (1994). Solid-State Redox Reactions of LiCoO2 (R$\bar{3}$m) for 4 Volt Secondary Lithium Cells. J Electrochem Soc *141*, 2972-2977.
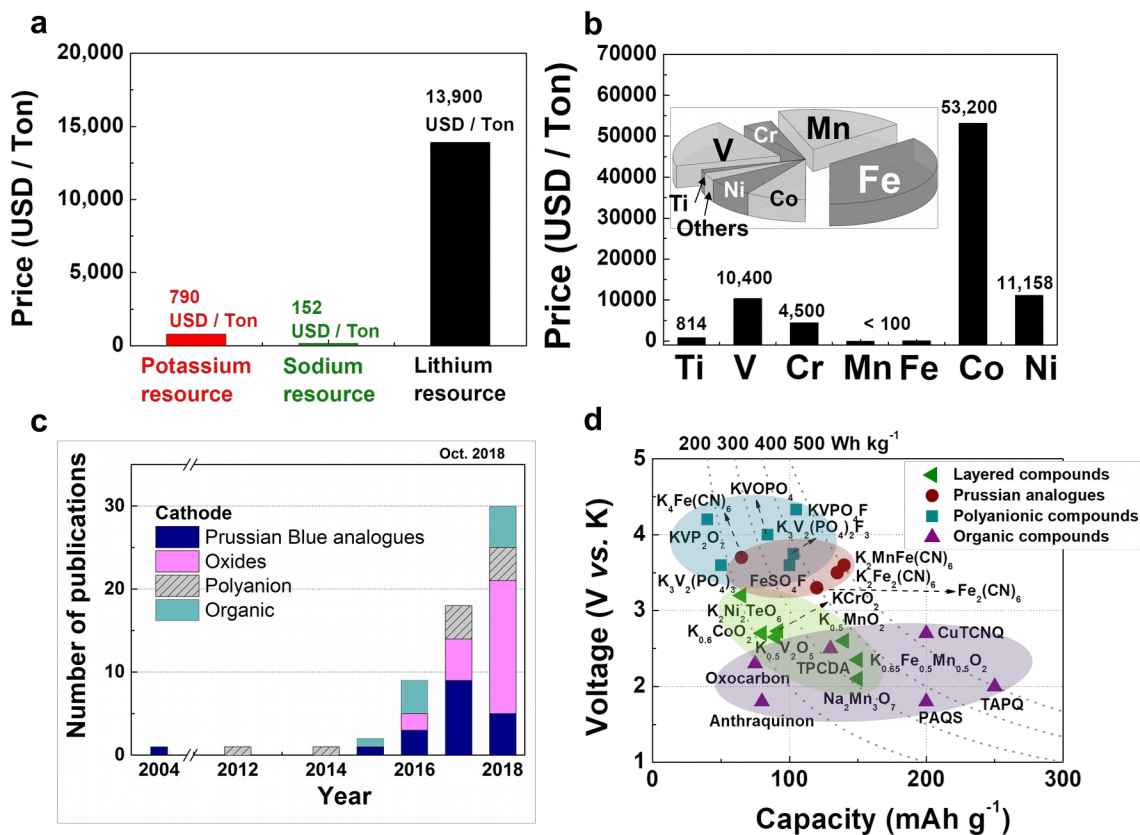
Figures

Figure 1. Price of alkali and transition metal elements that are used in alkali-ion cathode materials, number of publications and average voltage versus capacity diagram of various types of cathode materials for non-aqueous KIBs. (a) Price of potassium, sodium, and lithium resources. USGS Minerals Information: Commodity Statistics and Information Accessed October 2018. (b) Price of transition metal resources (Ti, V, Cr, Mn, Fe, Co, and Ni) and the relative occurrence of each transition metal in published K-ion cathodes (inset). USGS Minerals Information: Commodity Statistics and Information Accessed October 2018. (c) Number of publications per year on various cathode types. (Google Scholar. Accessed October 2018) (d) Capacity–voltage plots of K cathode compounds.
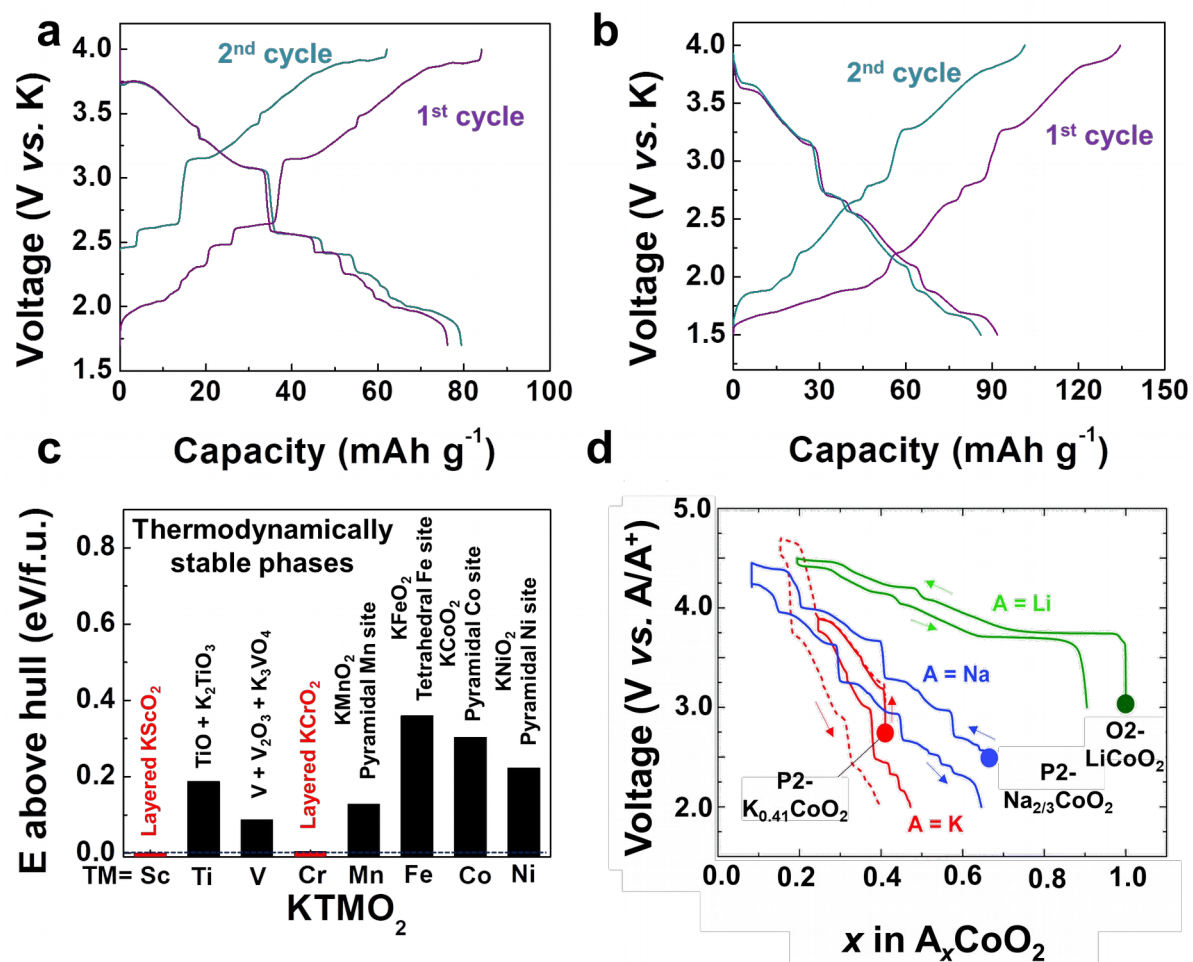
Figure 2. Charge-discharge profiles and computed stability of typical layered oxide compounds. (a) Charge–discharge profiles of P2-$K_{0.6}CoO_2$. Reproduced with permission [24]. Copyright 2017, WILEY-VCH. (b) Charge–discharge profiles of O3-$KCrO_2$. Reproduced with permission [27]. Copyright 2018, American Chemical Society. (c) Computed stability of layered KMO_2 compounds. Energy above the hull for various O3-layered compounds with KMO_2 stoichiometry. The height of the bar is the driving force for conversion to the more stable phases listed. Reproduced with permission [27]. Copyright 2018, American Chemical Society. (d) Comparison of charge–discharge

profiles for $K_{0.41}CoO_2$, $Na_{0.67}CoO_2$, and $LiCoO_2$. Reproduced with permission [25]. Copyright 2017, Royal Society of Chemistry.
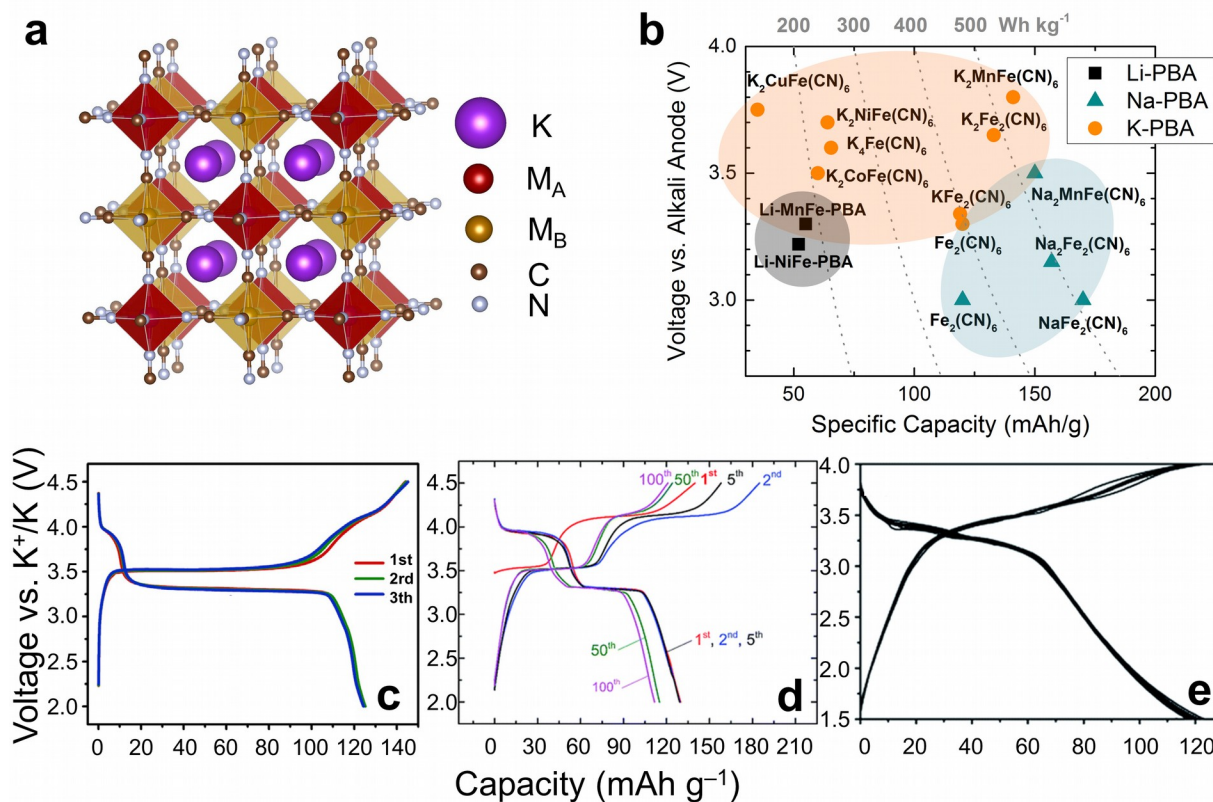

Figure 3. Crystal structure, average voltage versus gravimetric capacity, and voltage profiles of PBAs. (a) Crystal structure of PBAs. (b) Voltage–capacity relation of Li-, Na-, and K-PBA cathode materials [8-10, 33-39]. Voltage profiles of (c) $K_{0.61}Fe[Fe(CN)_6]_{0.91} \cdot 0.32H_2O$ Reproduced with permission [44]. Copyright 2018, Elsevier. (d) $K_{1.64}Fe[Fe(CN)_6]_{0.89} \cdot 0.15H_2O$. Reproduced with permission [34]. Copyright 2017, Royal Society of Chemistry. (e) a K-deficient $FeFe(CN)_6$ phase. Reproduced with permission [10]. Copyright 2017, Royal Society of Chemistry.
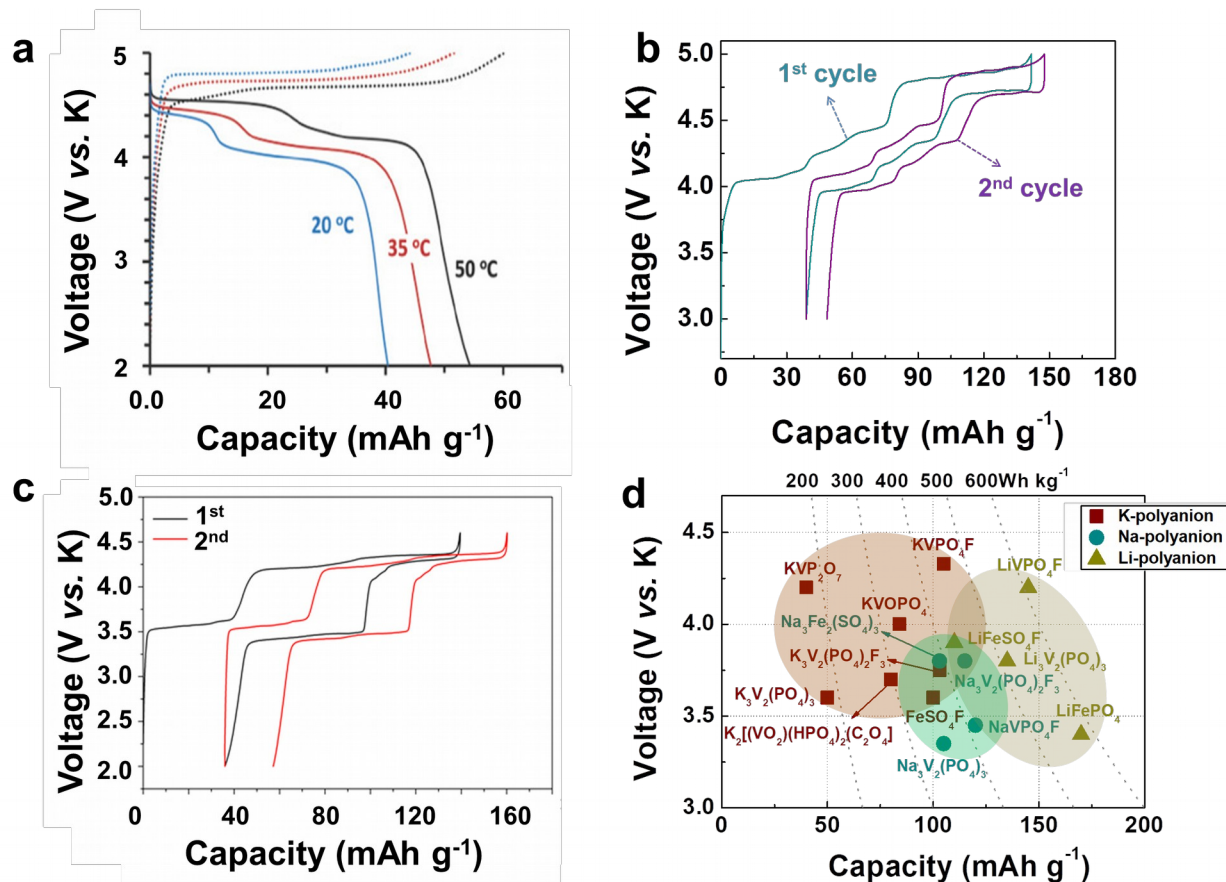
Figure 4. Charge–discharge profiles and capacity-voltage plot of K polyanionic compounds. (a) KVP_2O_7, reproduced with permission [47]. Copyright 2018, WILEY-VCH. (b) $KVPO_4F$, reproduced with permission [49]. Copyright 2018, WILEY-VCH (c) $K_3V_2(PO_4)_2F_3$, reproduced with permission [50]. Copyright 2019, Elsevier. (d) Voltage–capacity plots of Li-, Na-, and K-polyanion cathode materials [46-60].
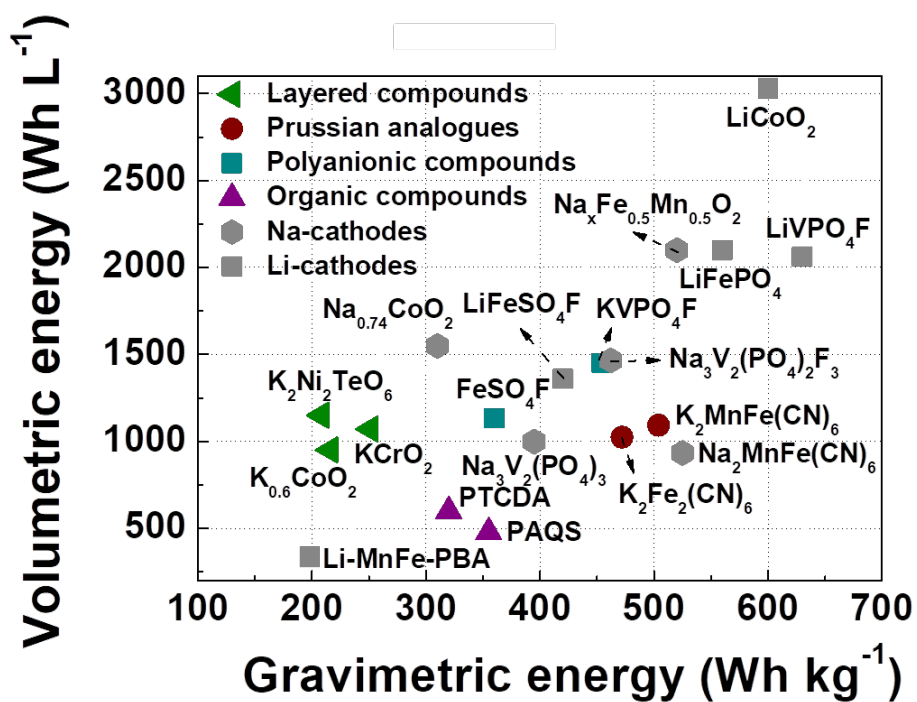
Figure 5. Gravimetric *vs.* volumetric energy density of K cathode compounds [11, 24, 26, 27, 35, 39, 46, 49, 57, 60, 61, 63, 66-71].